Electronic Supplementary Information

Dipyrrolyphenol as a precursor of π-electronic anion that forms ion pairs with cations

Hiromitsu Maeda,* Ayaka Fukui, Ryohei Yamakado and Nobuhiro Yasuda

College of Pharmaceutical Sciences, Ritsumeikan University, Kusatsu 525–8577, Japan, Tel: +81 77 561 5969; Fax: +81 77 561 2564; E-mail: maedahir@ph.ritsumei.ac.jp and Research and Utilization Division, Japan Synchrotron Radiation Research Institute, Sayo 679–5198, Japan.

Table of Contents

1. Synthetic procedures and spectroscopic data S2
Supporting Figure 1,2 ^{1}H and ^{13}C NMR of **1**. S3
2. X-ray crystallographic data S5
Supporting Figure 3–13 Single-crystal X-ray structures. S6
3. Optimization of molecular structures S16
Supporting Figure 14,15 Optimized structures and electron density diagrams. S16
Cartesian coordination of optimized structures S16
4. Deprotonation behaviors S20
Supporting Figure 16 UV/vis absorption spectral changes of **1** upon deprotonation in CH_2Cl_2. S20
Supporting Figure 17 ^{1}H NMR spectral changes of **1** upon deprotonation in CD_2Cl_2. S20
Supporting Figure 18 UV/vis absorption spectral changes upon pH titrations of **1** in an aqueous solution. S21

1. Synthetic procedures and spectroscopic data

General Procedures. Starting materials were purchased from Wako Pure Chemical Industries Ltd., Tokyo Chemical Industry Co., and Nacalai Tesque Inc., and used without further purification unless otherwise stated. UV-visible spectra were recorded on a Hitachi U-3500 spectrometer. NMR spectra used in the characterization of products were recorded on a JEOL ECA-600 600 MHz spectrometers. All NMR spectra were referenced to solvent. Matrix-assisted laser desorption ionization time-of-flight mass spectrometries (MALDI-TOF-MS) were recorded on a Shimadzu Axima-CFRplus using negative mode. TLC analyses were carried out on aluminum sheets coated with silica gel 60 (Merck 5554). Column chromatography was performed on Wakogel C-300.

4-Nitro-2,6-di(pyrrro-2-ly)phenol, 1. According to the related literature procedures,[S1] to a dried two-necked flask under a N_2 atmosphere, 1-(1,1-dimethylethoxy-carbonyl)pyrrole-2-boronic acid (509 mg, 2.41 mmol), 2,6-dibromo-4-nitrophenol (296 mg, 1.00 mmol), $Pd(OAc)_2$ (25.3 mg, 0.113 mmol), *t*-Bu_3P (115 μL, 0.475 mmol), and Na_2CO_3 (760 mg, 7.17 mmol) along with 1,2-dimethoxyethane (30 mL) and H_2O (2 mL) were added. The mixture was stirred at 90 °C for overnight and cooled to r.t. The mixture was acidified by the addition of dilute aqueous HCl, and the organic material was extracted with CH_2Cl_2. The organic layer was dried over Na_2SO_4 and the solvent was evaporated under vacuum. The crude product was purified with silica gel column chromatography (Wakogel C-300; eluent: CH_2Cl_2) and recrystallization from CH_2Cl_2/*n*-hexane to give **1** (75.4 mg, 0.280 mmol, 28%) as an orange solid. m.p.: 168 °C. R_f = 0.40 (CH_2Cl_2). ^{1}H NMR (600 MHz, $CDCl_3$, 20 °C): δ (ppm) 9.17 (s, 2H, NH), 8.23 (s, 2H, Ar-H), 7.24 (s, 1H, OH), 7.01 (m, 2H, pyrrole-H), 6.69 (m, 2H, pyrrole-H), 6.41 (dd, J = 3.6 and 3.0 Hz, 2H, pyrrole-H). ^{13}C NMR (151 MHz, $CDCl_3$, 20 °C): δ (ppm) 152.32, 142.36, 125.97, 121.43, 120.81, 120.66, 110.58, 108.68. MALDI-TOF-MS: *m/z* (% intensity): 268.1 (100). Calcd for $C_{14}H_{10}N_3O_3$ ($[M - H]^-$): 268.07. This compound was further characterized by single-crystal X-ray diffraction analysis.

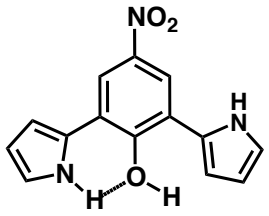

[S1] (a) A. F. Littke, C. Dai and G. C. Fu, *J. Am. Chem. Soc.*, 2000, **122**, 4020–4028; (b) H. Maeda, Y. Haketa and T. Nakanishi, *J. Am. Chem. Soc.*, 2007, **129**, 13661–13674.

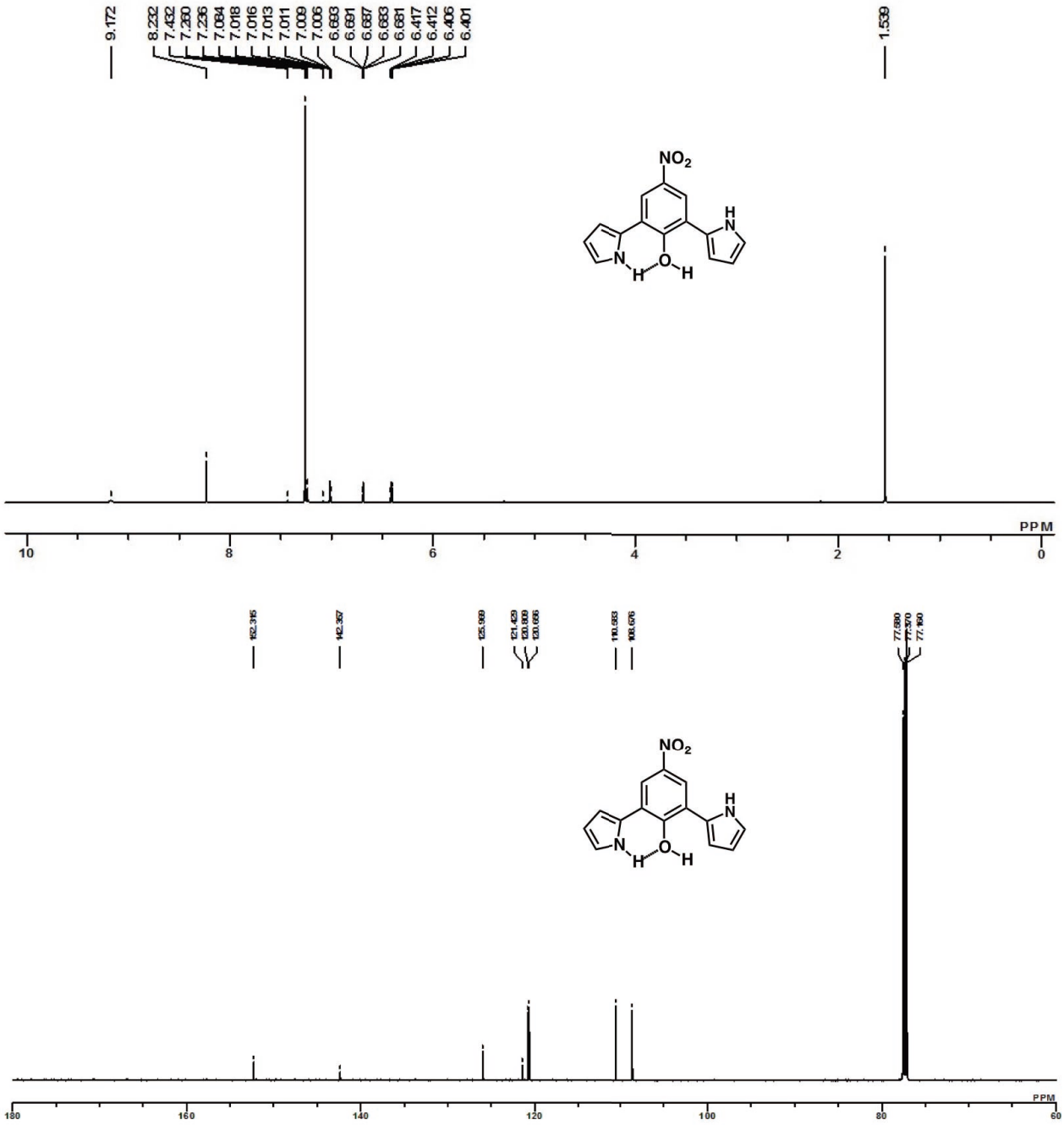

Supporting Figure 1 ^{1}H NMR (top) and ^{13}C NMR (bottom) spectra of **1** in $CDCl_3$.

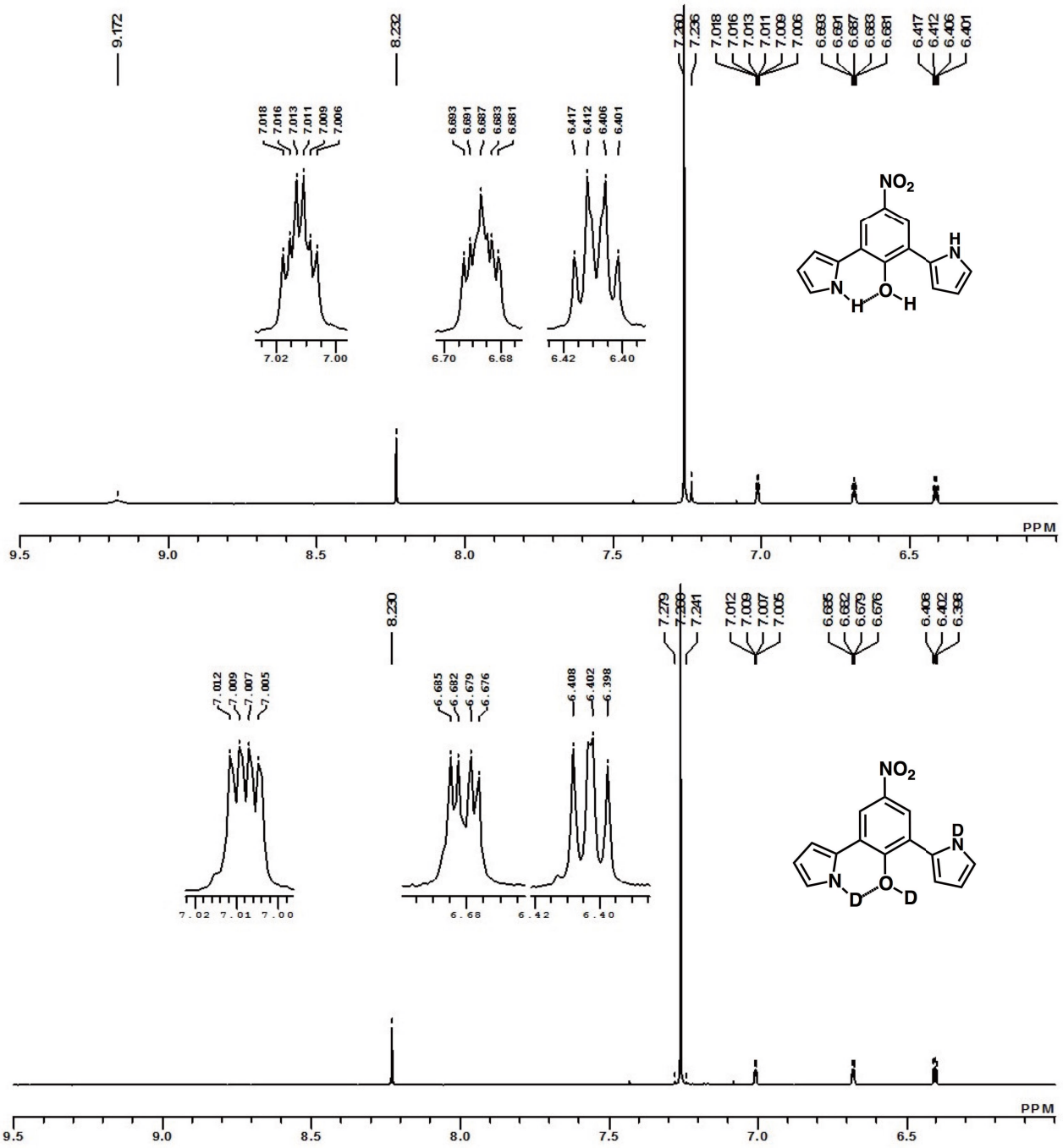

Supporting Figure 2 ^{1}H NMR spectral change of **1** in $CDCl_3$ upon the addition of a small amount of D_2O, resulting in the disappearance of the signal of pyrrole-NH along with phenol-OH and the corresponding changes of the coupling states of the pyrrole signals: before (top) and after (bottom) the addition of a small amount of D_2O. The signals with complicated coupling at 7.24 (s, 1H, OH), 7.01 (m, 2H, pyrrole-H), 6.69 (m, 2H, pyrrole-H), and 6.41 ppm (dd, J = 3.6 and 3.0 Hz, 2H, pyrrole-H), as a result of the three kinds of coupling, before H/D exchanges were changed to more clearly coupled signals with the exact assignment at 7.01 (dd, $J_{4,5}$ = 3.0 Hz, $J_{3,5}$ = 1.2 Hz, 2H, pyrrole-5H), 6.69 (dd, $J_{3,4}$ = 3.3 Hz, $J_{3,5}$ = 1.2 Hz, 2H, pyrrole-3H), and 6.41 ppm (dd, $J_{3,4}$ = 3.3 Hz, $J_{4,5}$ = 3.0 Hz, 2H, pyrrole-4H), respectively.

2. X-ray crystallographic data

Method for single-crystal X-ray analysis: Crystallographic data for **1**, **1**$^{-}$-TPA^{+}, **1**$^{-}$-TBA^{+}, **1**$^{-}$-15-crown-5·Na^{+}, **1**$^{-}$-18-crown-6·K^{+}, and **1**$^{-}$-DMAP·H^{+} are summarized in Supporting Table 1. A single crystal of **1** was obtained by vapor diffusion of *n*-hexane into a CH_2Cl_2 solution of **1**. The data crystal was a yellow prism of approximate dimensions 0.25 mm × 0.07 mm × 0.01 mm. Data were collected at 93(2) K on a Rigaku XtaLAB P200 diffractometer with graphite monochromated Cu-Kα radiation (λ = 1.54187 Å). A single crystal of **1**$^{-}$-TBA^{+} was obtained by vapor diffusion of *n*-hexane into a THF solution of **1** and excess tetrabutylammonium hydroxide (TBAOH). The data crystal was a red prism of approximate dimensions 0.16 mm × 0.09 mm × 0.01 mm. Data were collected at 93(2) K on a Rigaku RAXIS-RAPID II diffractometer with graphite monochromated Cu-Kα radiation (λ = 1.54187 Å). A single crystal of **1**$^{-}$-TPA^{+} was obtained by vapor diffusion of *n*-hexane into a THF solution of **1** and 1 equiv of tetrapropylammonium hydroxide (TPAOH). The data crystal was a red prism of approximate dimensions 0.80 mm × 0.10 mm × 0.10 mm. Data were collected at 93(2) K on a Rigaku RAXIS-RAPID II diffractometer with graphite monochromated Cu-Kα radiation (λ = 1.54187 Å). A single crystal of **1**$^{-}$-15-crown-5·Na^{+} was obtained by vapor diffusion of *n*-hexane into a THF solution of **1** with an excess amount of a 1:1 mixture of NaOH and 15-crown-5-ether. The data crystal was a red prism of approximate dimensions 0.32 mm × 0.10 mm × 0.02 mm. Data were collected at 93(2) K on a Rigaku XtaLAB P200 diffractometer with graphite monochromated Cu-Kα radiation (λ = 1.54187 Å). A single crystal of **1**$^{-}$-18-crown-6·K^{+} was obtained by vapor diffusion of *n*-hexane into a CH_2Cl_2 solution of **1** with an excess amount of a 1:1 mixture of KOH and 18-crown-6-ether. The data crystal was a red needle of approximate dimensions 0.04 mm × 0.02 mm × 0.003 mm. Data were collected at 100(2) K on a Rigaku Saturn 724 diffractometer with Si (111) monochromated synchrotron radiation (λ = 0.78203 Å) at BL40XU (SPring-8).[S2] A single crystal of **1**$^{-}$-DMAP·H^{+} was obtained by vapor diffusion of *n*-hexane into a CH_2Cl_2 solution of **1** with a mixture of 1 equiv of 4-dimethylaminopyridine (DMAP). The data crystal was a red prism of approximate dimensions 0.49 mm × 0.10 mm × 0.04 mm. Data were collected at 93(2) K on a Rigaku XtaLAB P200 diffractometer with graphite monochromated Cu-Kα radiation (λ = 1.54187 Å). In each case, the structure was solved by direct method and the non-hydrogen atoms were refined anisotropically except for the oxygen of a water as the solvent molecule in **1**$^{-}$-18-crown-6·K^{+}. The calculations were performed using the Crystal Structure crystallographic software package of Molecular Structure Corporation.[S3] CIF files (CCDC 1420539–1420544) can be obtained free of charge from the Cambridge Crystallographic Data Centre via www.ccdc.cam.ac.uk/data_request/cif.

Supporting Table 1 Crystallographic details for compounds **1**, **1**$^{-}$-TPA^{+}, **1**$^{-}$-TBA^{+}, **1**$^{-}$-15-crown-5·Na^{+}, **1**$^{-}$-18-crown-6·K^{+}, and **1**$^{-}$-DMAP·H^{+}.

	1	**1**$^{-}$-TBA^{+}	**1**$^{-}$-TPA^{+}	**1**$^{-}$-15-crown-5·Na^{+}	**1**$^{-}$-18-crown-6·K^{+}	**1**$^{-}$-DMAP·H^{+}
formula	$C_{14}H_{11}N_3O_3$	$C_{14}H_{10}N_3O_3^{-}\cdot C_{16}H_{36}N^{+}$	$C_{14}H_{10}N_3O_3^{-}\cdot C_{12}H_{28}N^{+}$	$C_{14}H_{10}N_3O_3^{-}\cdot C_{10}H_{20}O_5\cdot Na^{+}$	$C_{14}H_{10}N_3O_3^{-}\cdot C_{12}H_{24}O_6\cdot K^{+}\cdot H_2O$	$C_{14}H_{10}N_3O_3^{-}\cdot C_7H_{11}N_2^{+}$
fw	269.26	510.71	454.60	511.50	589.68	391.43
crystal size, mm	0.25 × 0.07× 0.01	0.16 × 0.09 × 0.01	0.80 × 0.10 × 0.10	0.32 × 0.10 × 0.02	0.04 × 0.02 × 0.003	0.49 × 0.10 × 0.04
crystal system	monoclinic	monoclinic	monoclinic	monoclinic	triclinic	monoclinic
space group	$P2_1/n$ (no.14)	$P2_1/c$ (no. 14)	$P2_1/c$ (no. 14)	$P2_1/c$ (no. 14)	P-1 (no. 2)	$P2_1/c$ (no. 14)
a, Å	10.342(6)	18.1094(17)	16.8579(5)	7.916(3)	10.778(3)	9.516(3)
b, Å	6.841(6)	8.5397(8)	8.6583(3)	16.599(6)	10.915(3)	16.738(5)
c, Å	17.218(10)	19.1583(17)	18.4879(5)	18.426(6)	14.506(4)	12.250(3)
α, °	90	90	90	90	82.963(5)	90
β, °	102.267(15)	105.390(5)	111.4165(15)	94.920(6)	86.231(4)	107.800(8)
γ, °	90	90	90	90	63.226(7)	90
V, Å^3	1190.4(12)	2856.6(5)	2512.18(13)	2412.2(15)	1512.0(7)	1857.8(9)
ρ_{calcd}, gcm^{-3}	1.502	1.188	1.202	1.408	1.295	1.399
Z	4	4	4	4	2	4
T, K	93(2)	93(2)	93(2)	93(2)	100(2)	93(2)
μ (Cu-Kα), mm^{-1}	0.906	0.606	0.632	1.039	0.297 [a]	0.792
no. of reflns	7902	28318	25534	15581	11255	12001
no. of unique reflns	2041	4566	4368	4116	5121	3264
variables	182	334	298	325	370	264
$\lambda_{Mo\text{-}K\alpha}$, Å	1.54187	1.54187	1.54187	1.54187	0.78291 [a]	1.54187
R_1 ($I > 2\sigma(I)$)	0.0533	0.0853	0.0556	0.0414	0.0556	0.0329
wR_2 ($I > 2\sigma(I)$)	0.1592	0.2005	0.1129	0.1099	0.1435	0.0929
GOF	1.031	1.013	1.011	1.019	0.965	1.071

[a] The values under the synchrotron radiation.

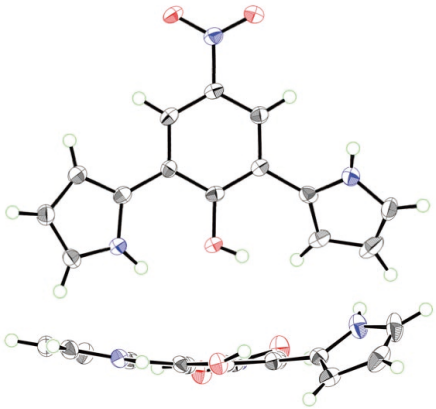

Supporting Figure 3 Ortep drawing of single-crystal X-ray structure (top and side views) of **1**, wherein thermal ellipsoids are scaled to the 50% probability level and atom color code: black, green, blue, and red refer to carbon, hydrogen, nitrogen, and oxygen, respectively. Dihedral angles of the inverted pyrrole and non-inverted pyrrole units to the core unit were estimated as 8.88°/37.25°, respectively. Pyrrole inversion induced the intramolecular N–H···O hydrogen bonding with the N(–H)···O distance of 2.64 Å.

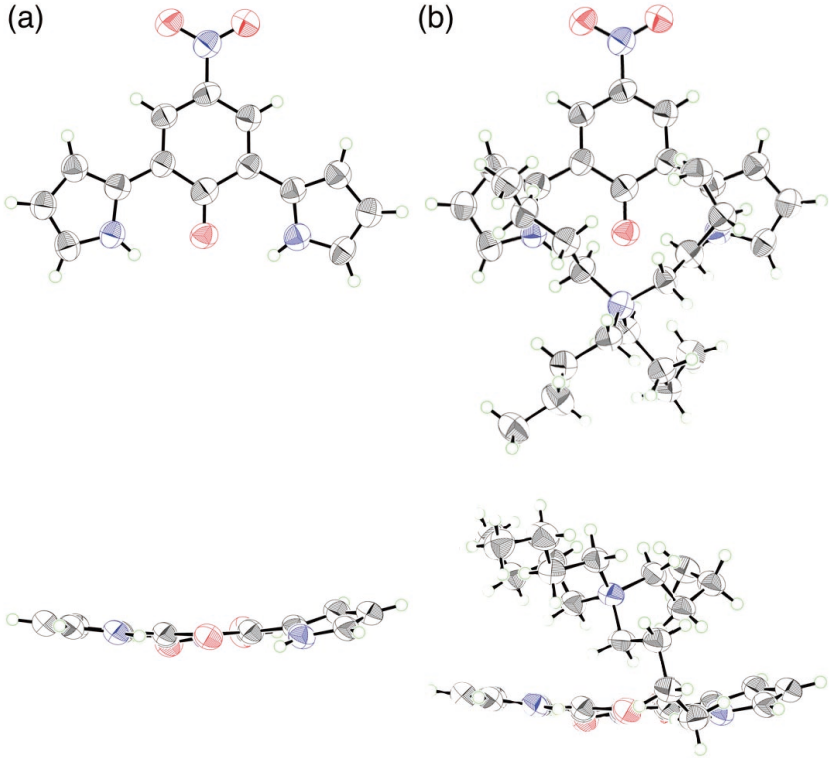

Supporting Figure 4 Ortep drawing of single-crystal X-ray structures (top and side views) of $\mathbf{1}^{-}$-TBA^{+} as (a) the anion part and (b) the ion-pairing form, wherein thermal ellipsoids are scaled to the 50% probability level and atom color code: black, green, blue, and red refer to carbon, hydrogen, nitrogen, and oxygen, respectively. In the solid state, $\mathbf{1}^{-}$ formed intramolecular hydrogen bonding between two pyrrole NH and phenolate oxygen with the N(–H)···O distances of 2.68 and 2.70 Å, giving more planar structures compared to **1** as seen in the dihedral angles of 8.77° and 18.92° for the pyrrole units to the core unit in $\mathbf{1}^{-}$. The distance between TBA^{+} nitrogen and phenolate oxygen is 4.12 Å, whereas those between TBA^{+} carbons adjacent to the nitrogen and phenolate oxygen are estimated as 3.60, 3.72, 4.36, and 5.60 Å.

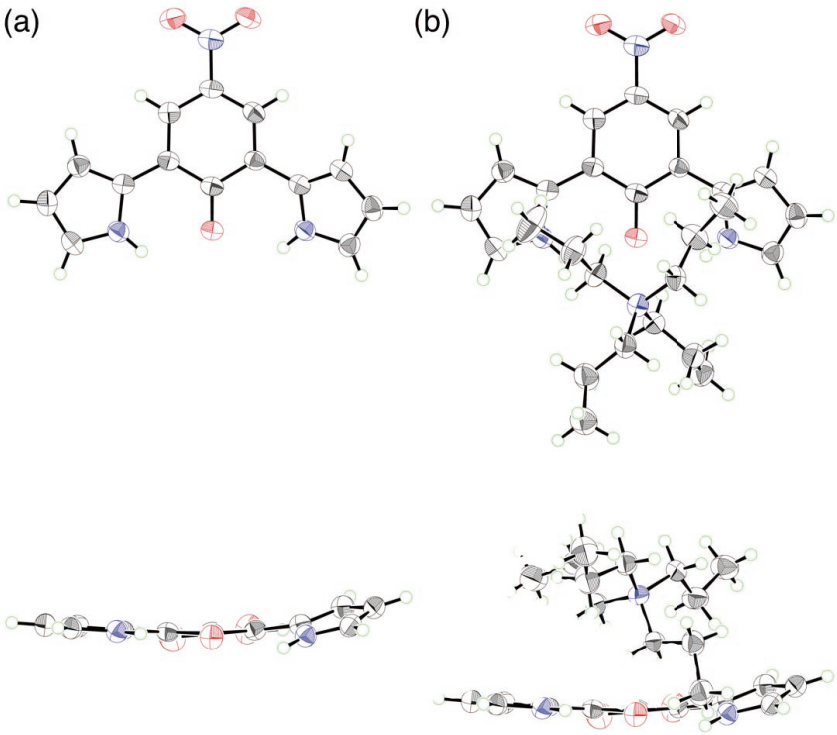

Supporting Figure 5 Ortep drawing of single-crystal X-ray structures (top and side views) of $\mathbf{1}^{-}$-TPA^{+} as (a) the anion part and (b) the ion-pairing form, wherein thermal ellipsoids are scaled to the 50% probability level and atom color code: black, green, blue, and red refer to carbon, hydrogen, nitrogen, and oxygen, respectively. In the solid state, $\mathbf{1}^{-}$ formed intramolecular hydrogen bonding between two pyrrole NH and phenolate oxygen with the N(–H)···O distances of 2.68 and 2.67 Å, giving more planar structures compared to **1** as seen in the dihedral angles of 5.63° and 22.00° for the pyrrole units to the core unit in $\mathbf{1}^{-}$. The distance between TPA^{+} nitrogen and phenolate oxygen is 3.96 Å, whereas those between TBA^{+} carbons adjacent to the nitrogen and phenolate oxygen are estimated as 3.26, 3.54, 4.47, and 5.36 Å.

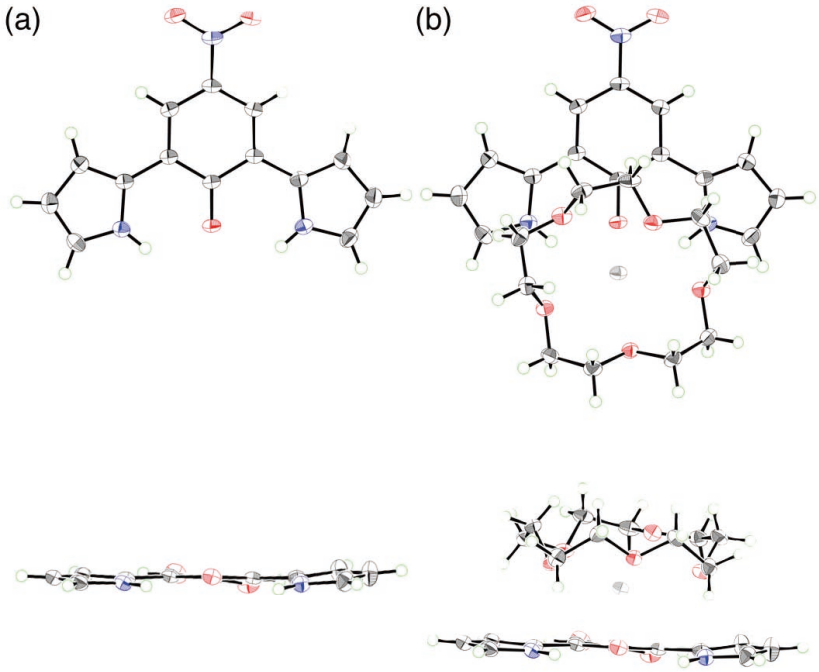

Supporting Figure 6 Ortep drawing of single-crystal X-ray structures (top and side views) of $\mathbf{1}^{-}$-15-crown-5·Na^{+} as (a) the anion part and (b) the ion-pairing form, wherein thermal ellipsoids are scaled to the 50% probability level and atom color code: black, green, blue, red, and gray refer to carbon, hydrogen, nitrogen, oxygen, and sodium, respectively. In the solid state, $\mathbf{1}^{-}$ formed intramolecular hydrogen bonding between two pyrrole NH and phenolate oxygen with the N(–H)···O distances of 2.64 and 2.66 Å, giving more planar structures compared to **1** as seen in the dihedral angles of 5.74° and 10.91° for the pyrrole units to the core unit in $\mathbf{1}^{-}$. The distance between Na^{+} and phenolate oxygen is estimated as 2.35 Å.

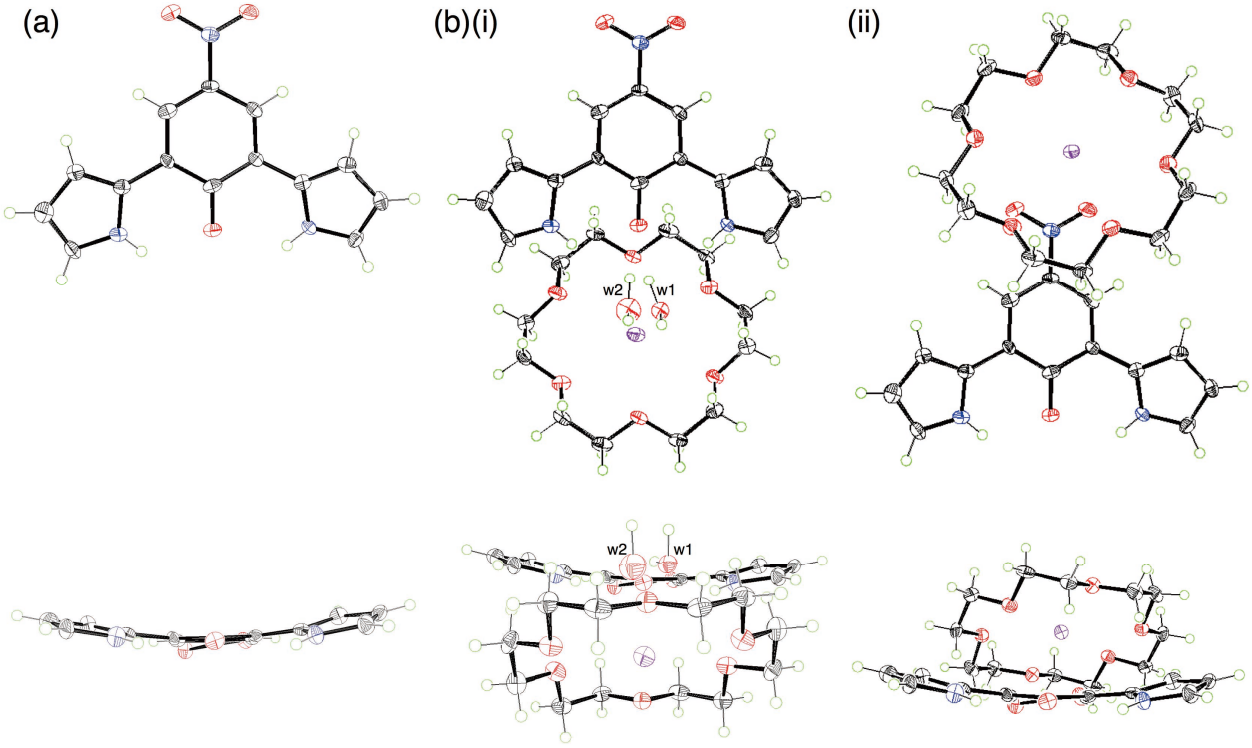

Supporting Figure 7 Ortep drawing of single-crystal X-ray structures (top and side views) of $\mathbf{1}^{-}$-18-crown-6·K^{+} as (a) the anion part and (b) two kinds of the ion-pairing forms containing independent 18-crown-6·K^{+} parts. In (b)(i), disordered structures were observed at the water included as the solvent molecule in the ratio of 0.819:0.181 (w1 : w2). Thermal ellipsoids are scaled to the 50% probability level and atom color code: black, green, blue, red, and purple refer to carbon, hydrogen, nitrogen, oxygen, and potassium, respectively. In the solid state, $\mathbf{1}^{-}$ formed intramolecular hydrogen bonding between two pyrrole NH and phenolate oxygen with the N(–H)···O distances of 2.73 and 2.81 Å, giving more planar structures compared to $\mathbf{1}^{-}$ as seen in the dihedral angles of 13.96° and 17.05° for the pyrrole units to the core unit in $\mathbf{1}^{-}$. H_2O oxygen (w1) and phenolate oxygen formed the hydrogen bonding with the O(–H)···O distances of 2.77 Å, whereas those between NO_2 oxygen and K^{+} are estimated as 2.88 Å.

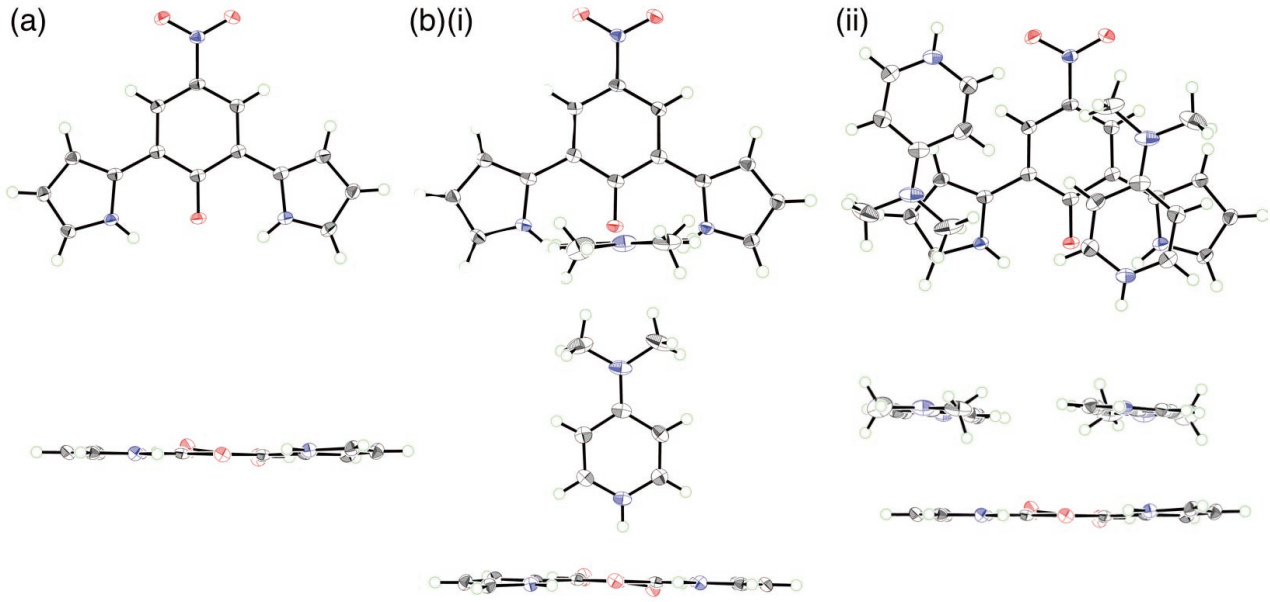

Supporting Figure 8 Ortep drawing of single-crystal X-ray structures (top and side views) of $\mathbf{1}^{-}$-DMAP·H^{+} as (a) the anion part and (b) three kinds of the ion-pairing forms, wherein thermal ellipsoids are scaled to the 50% probability level and atom color code: black, green, blue, and red refer to carbon, hydrogen, nitrogen, and oxygen, respectively. In the solid state, $\mathbf{1}^{-}$ formed intramolecular hydrogen bonding between two pyrrole NH and phenolate oxygen with the N(–H)···O distances of 2.65 and 2.66 Å, giving more planar structures compared to **1** as seen in the dihedral angles of 0.83°/5.02° for the pyrrole units to the core unit in $\mathbf{1}^{-}$-DMAP·H^{+}. The dihedral angle of one the combination of $\mathbf{1}^{-}$ and DMAP·H^{+} is 94.7° (for the phenyl moiety of $\mathbf{1}^{-}$) and 93.5° (for the mean plane consisting of 16 core atoms of $\mathbf{1}^{-}$) through the hydrogen bonding between NH of DMAP·H^{+} and anionic oxygen in $\mathbf{1}^{-}$ with the N(–H)···O^{-} distance of 2.47 Å (b)(i). The dihedral angles of the other combinations of $\mathbf{1}^{-}$ and DMAP·H^{+} is 2.64° (for the phenyl moiety of $\mathbf{1}^{-}$) and 3.93° (for the mean plane consisting of 16 core atoms of $\mathbf{1}^{-}$) and the π-plane distances of 3.20 and 3.40 Å (for the phenyl moiety of $\mathbf{1}^{-}$) and 3.30 and 3.35 Å (for the mean plane consisting of 16 core atoms of $\mathbf{1}^{-}$) as observed in (b)(ii).

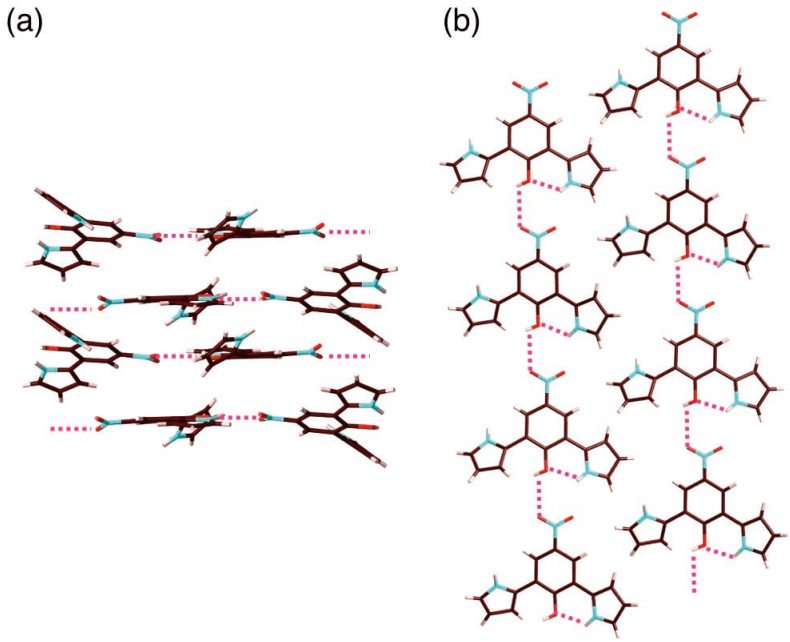

Supporting Figure 9 Packing diagrams of **1**, wherein atom color code: brown, pink, blue, and red refer to carbon, hydrogen, nitrogen, and oxygen, respectively. Intermolecular hydrogen bonding was observed between phenol OH and NO_2 oxygen with the O(–H)···O distance of 2.97 Å.

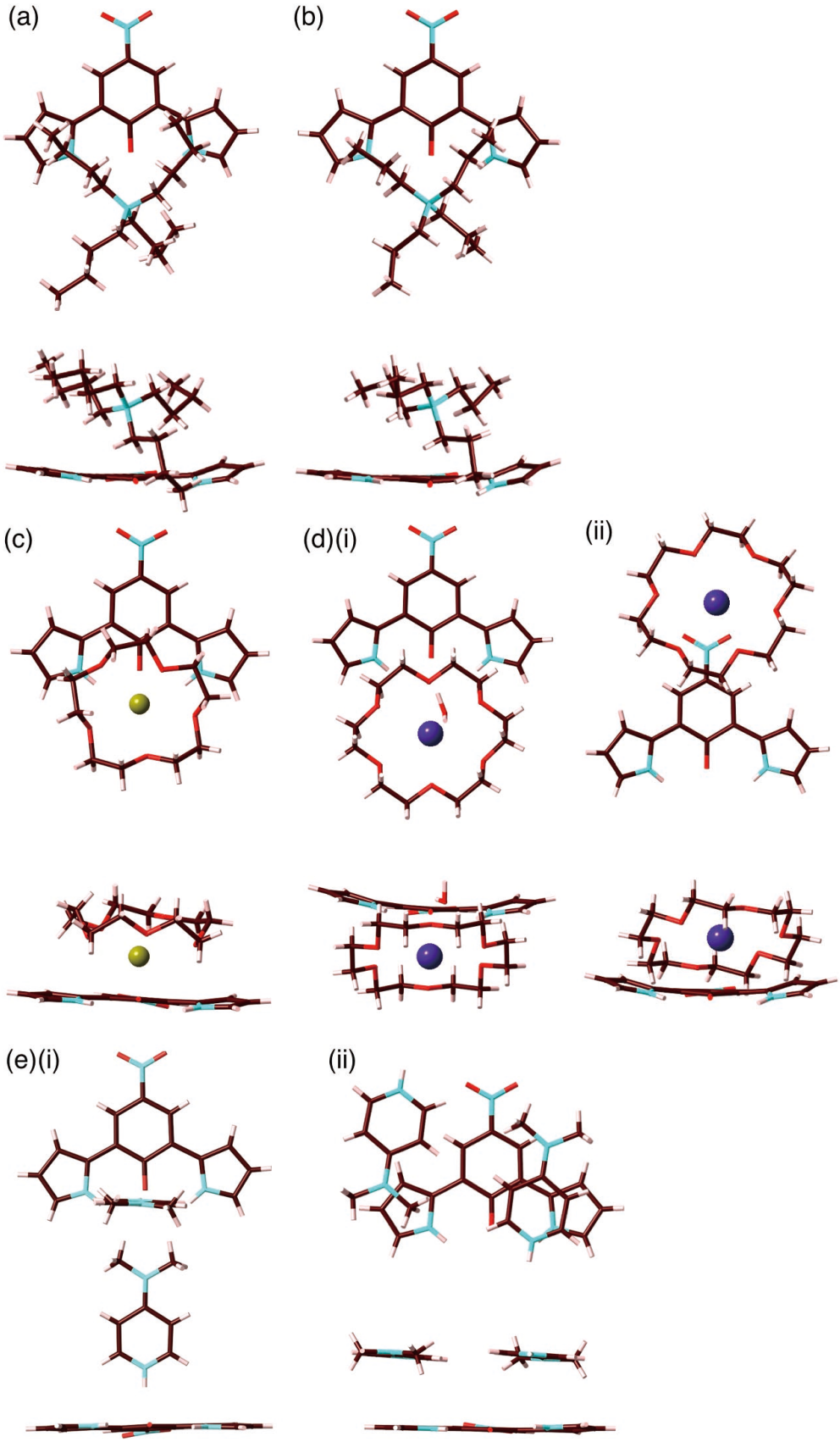

Supporting Figure 10 Solid-state ion-pairing structures (top and side views) of (a) $\mathbf{1}^{-}$-TBA^{+}, (b) $\mathbf{1}^{-}$-TPA^{+}, (c) $\mathbf{1}^{-}$-15-crown-5·Na^{+}, (d) $\mathbf{1}^{-}$-18-crown-6·K^{+} as two kinds of ion-pairing forms, and (e) $\mathbf{1}^{-}$-DMAP·H^{+} as three kinds of ion-pairing forms. Atom color code: brown, pink, blue, red, yellow, and purple refer to carbon, hydrogen, nitrogen, oxygen, sodium, and potassium, respectively.

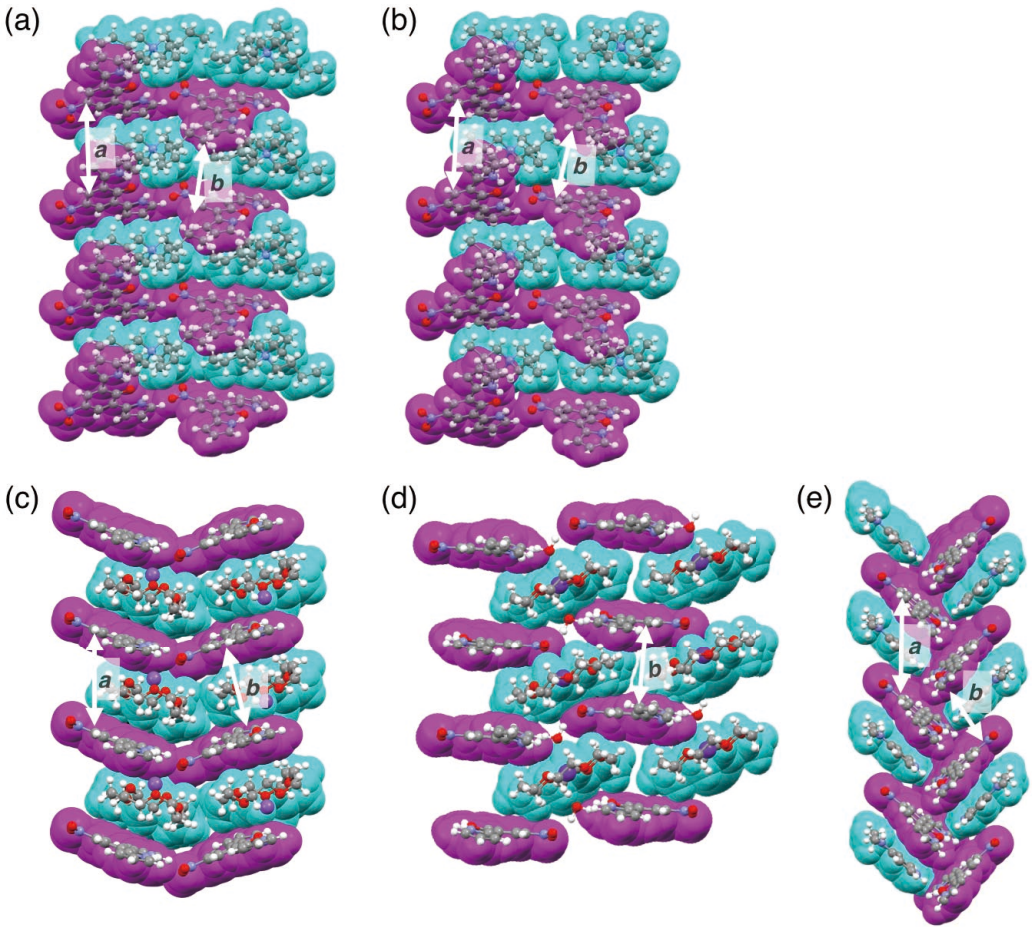

Supporting Figure 11 Solid-state charge-by-charge stacking structures of **1**$^{-}$-TBA^{+} (a = 8.41 Å, b = 7.27 Å), (b) **1**$^{-}$-TPA^{+} (a = 8.66 Å, b = 7.46 Å), (c) **1**$^{-}$-15-crown-5·Na^{+} (a = 7.92 Å, b = 7.27 Å), (d) **1**$^{-}$-18-crown-6·K^{+} (b = 7.41 Å) and (e) **1**$^{-}$-DMAP·H^{+} (a = 6.95 Å, b = 6.26 Å), wherein color codes of cyan and magenta in the space-filling models refer to **1**$^{-}$ and the corresponding cations (TPA^{+}, TBA^{+}, 15-crown-5·Na^{+}, 18-crown-6·K^{+}, and DMAP·H^{+}), respectively. The parameter a represents the distance between the aryl C4 positions in the neighboring **1**$^{-}$, whereas the parameter b represents the distance between the neighboring mean planes of **1**$^{-}$ consisting of the 16 core atoms. For the assembly in (d) **1**$^{-}$-18-crown-6·K^{+}, the detailed structure exhibiting the specific interactions is shown in Supporting Figure 12.

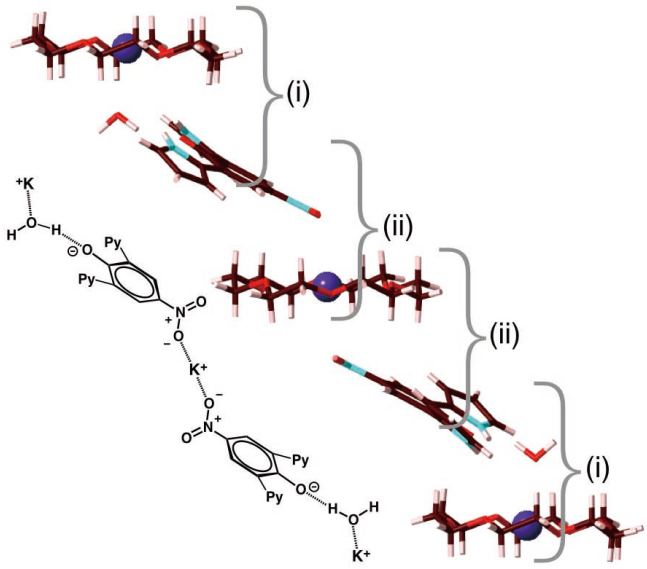

Supporting Figure 12 Packing structure exhibiting the specific interactions and the corresponding schematic representation of $\mathbf{1}^{-}$-18-crown-6·K^{+}, wherein atom color code: brown, pink, blue, red, and purple refer to carbon, hydrogen, nitrogen, oxygen, and potassium, respectively. The ion-pairing parts labeled by (i) and (ii) in the packing structure correspond to those in the Supporting Figure 10d.

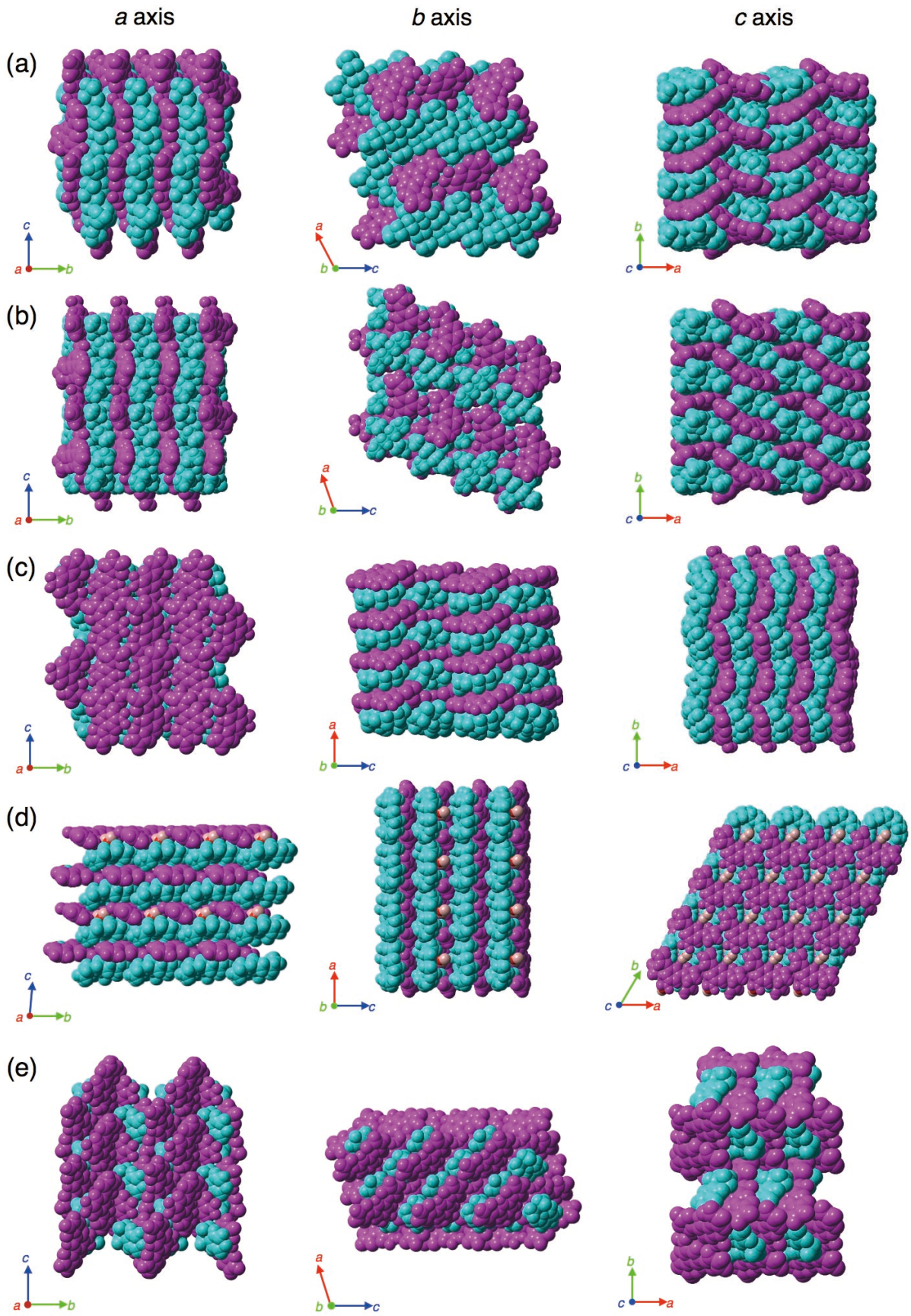

Supporting Figure 13 Packing diagrams through *a*, *b*, and *c* axes of (a) $\mathbf{1}^{-}$-TBA^{+}, (b) $\mathbf{1}^{-}$-TPA^{+}, (c) $\mathbf{1}^{-}$-15-crown-5·Na^{+}, (d) $\mathbf{1}^{-}$-18-crown-6·K^{+}, and (e) $\mathbf{1}^{-}$-DMAP·H^{+}, wherein color codes of cyan and magenta in the space-filling models refer to $\mathbf{1}^{-}$, the corresponding cations (TPA^{+}, TBA^{+}, 15-crown-5·Na^{+}, 18-crown-6·K^{+}, and DMAP·H^{+}), respectively, and those of pink and red are hydrogen and oxygen parts, respectively, of water molecules.

[S2] (a) N. Yasuda, H. Murayama, Y. Fukuyama, J. E. Kim, S. Kimura, K. Toriumi, Y. Tanaka, Y. Moritomo, Y. Kuroiwa, K. Kato, H. Tanaka and M. Takata, *J. Synchrotron Rad.*, 2009, **16**, 352–357; (b) N. Yasuda, Y. Fukuyama, K. Toriumi, S. Kimura and M. Takata, *AIP Conf. Proc.*, 2010, **1234**, 147–150.

[S3] *CrystalStructure (Ver. 3.8), Single Crystal Structure Analysis Software,* Rigaku/MSC and Rigaku Corporation, 2006.

3. Optimization of molecular structures

DFT calculations. Ab initio calculations of the geometrical optimizations and estimation of electrostatic potentials of **1** and the anion form $\mathbf{1}^-$ were carried out by using the *Gaussian 09* program.[S4]

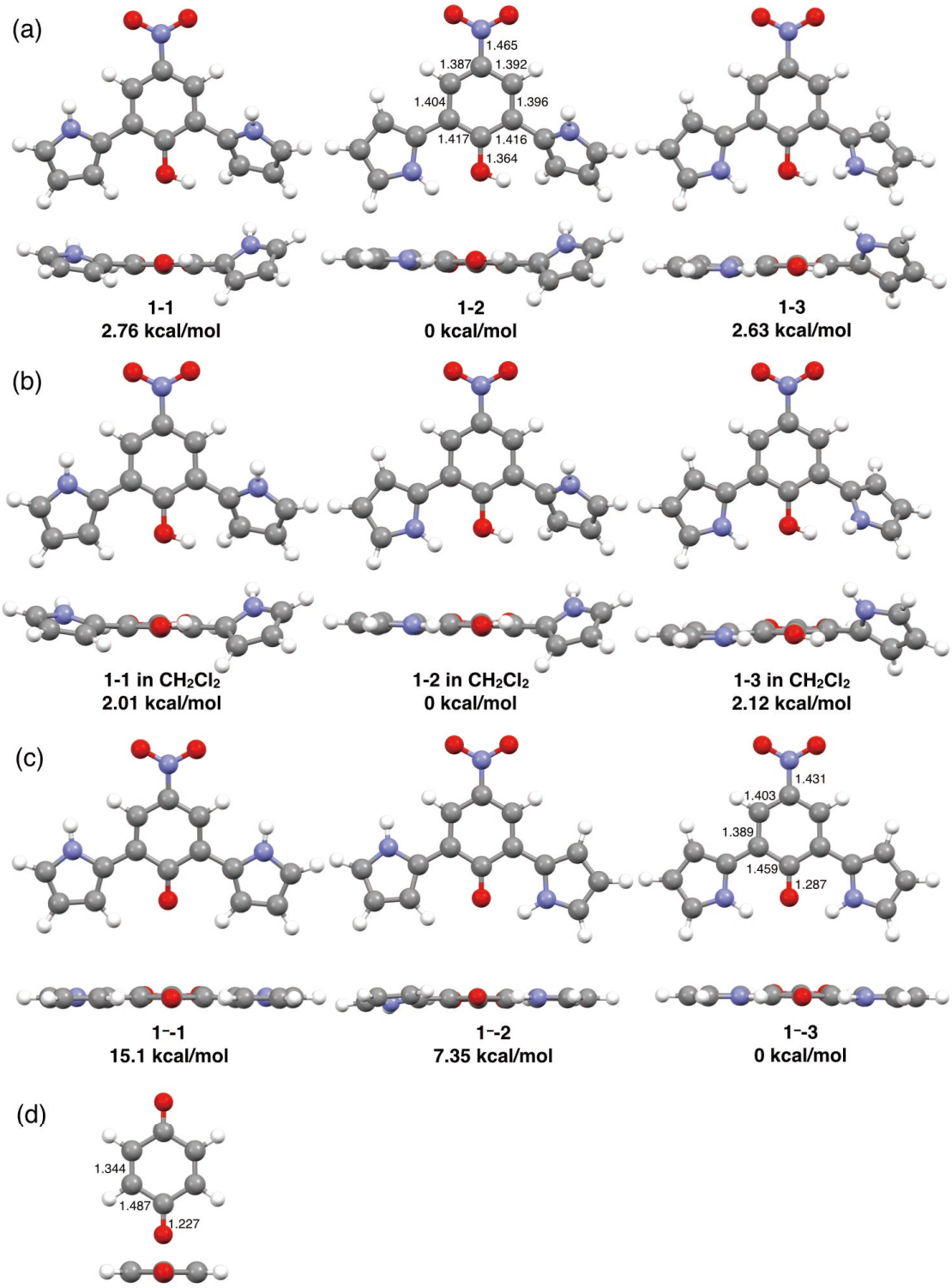

Supporting Figure 14 Optimized structures (top and side views) of (a) **1** at B3LYP/6-31G(d,p), (b) **1** at B3LYP/6-31+G(d,p)//B3LYP/6-31G(d,p) in CH_2Cl_2 using the SCIPCM method, (c) $\mathbf{1}^-$ at B3LYP/6-31+G(d,p), and (d) *p*-benzoquinone, as a reference species, at B3LYP/6-31G(d,p). The contribution of the quinoid resonance structure in the anionic form $\mathbf{1}^-$ was suggested by the observation of the bond lengths such as 1.46, 1.39, 1.40, and 1.29 Å for C^1–C^2, C^2–C^3, C^3–C^4, and C^1–O, respectively, wherein the superscript numbers correspond to the locations at the phenolate unit.

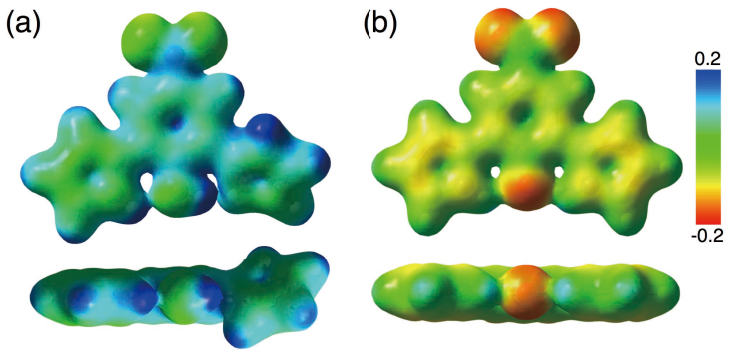

Supporting Figure 15 Electron density diagrams of (a) **1** as the singly pyrrole-inverted conformation (most stable conformation of **1**) and (b) $\mathbf{1}^{-}$ as the pyrrole-inverted conformation (most stable conformation of $\mathbf{1}^{-}$) estimated by electrostatic potential mapped onto the electron density isosurface (δ = 0.02) calculated at (a) B3LYP/6-31+G(d,p)//B3LYP/6-31G(d,p) level and (b) B3LYP/6-31+G(d,p). Electrostatic potential (ESP) mapping of $\mathbf{1}^{-}$ showed the delocalization of the negative charge on the π-conjugated moiety and nitro oxygen atoms.

Cartesian Coordination of 1-1

-929.9554295 hartree

C,-1.4357073,0.05309376,-2.21962225
C,-1.14149458,-0.27774065,4.69388272
C,-0.19611222,-0.03373248,2.63865514
C,-0.42871735,-0.03442178,-1.16512616
C,0.93366598,-0.11987791,-1.48136082
C,0.20683048,-0.07506335,1.22718378
C,-0.77814647,-0.01259761,0.21048826
C,1.89771357,-0.14753221,-0.47875344
C,-3.26668204,-0.00353671,-3.56482225
C,-2.80012018,-0.2177308,-2.24404034
C,-0.06452933,0.57271598,4.81082691
C,-1.23219133,-0.66042549,3.32733963
C,1.55613469,-0.13381816,0.86877883
C,-2.18791163,0.40320748,-4.32303978
H,-4.27870855,-0.13204693,-3.92111642
H,-0.18094835,0.76827337,-3.78276597
H,2.33537341,-0.20469728,1.61681803
H,-2.1166382,0.68318113,-5.36345868
H,1.26541822,1.32618802,3.33843622
H,-1.78550083,-0.60056699,5.49897031
H,0.34028496,1.0897847,5.66766999
H,-3.37999328,-0.55028697,-1.39897141
H,1.27027926,-0.18899783,-2.50757609
H,-1.91617764,-1.38573059,2.90741734
H,-2.16118852,0.22560604,1.48994747
N,-1.08669215,0.42334143,-3.5094168
N,0.50252936,0.70828187,3.56800229
N,3.30929773,-0.22242937,-0.8531405
O,4.14538611,-0.23858042,0.05344339
O,3.58744163,-0.25777466,-2.05424302
O,-2.08839511,0.08756699,0.52757125

Cartesian Coordination of 1-2

-929.9598267 hartree

C,-1.0093091283,0.014736818,-2.4054454573
C,-0.8734736883,-0.2789774835,4.8467290192
C,-0.5340301819,-0.1347951769,2.6048295704
C,-0.162200596,0.0789235247,-1.2068214868
C,1.2217766865,0.229685355,-1.3136381526
C,0.0288872342,-0.0079033963,1.2625412469
C,-0.7452276628,-0.0512200146,0.0762689347
C,1.9851324474,0.2589624785,-0.1507003746
C,-2.5977332258,0.1981036787,-4.0246310984
C,-2.2489172918,0.5789995973,-2.6993667124
C,-2.0979454552,-0.374542891,4.2110023171
C,0.1094853815,-0.1289838117,3.8420951599
C,1.4147632793,0.1553708637,1.1105655993
C,-1.5758064075,-0.5889277771,-4.5071386167
H,-3.4894334339,0.481746192,-4.5645759562
H,0.2099266279,-1.2577734194,-3.5741301056
H,2.0634441914,0.1986178415,1.9743974553
H,-1.4511561,-1.0836283159,-5.4585141174
H,-2.5789693221,-0.330846059,2.1385868291
H,-0.7074315214,-0.3133643653,5.9138323831
H,-3.0939160025,-0.4975677574,4.609655035
H,-2.7904551729,1.2684051759,-2.0654154244
H,1.7043223529,0.3552241533,-2.2742140746
H,1.1727249604,-0.0274605362,4.0043123339
H,-2.4611352205,-0.3714678763,-0.7003559768
N,-0.6210591337,-0.6886855102,-3.5257990087
N,-1.8829048044,-0.2860598135,2.8659863832
N,3.4375713802,0.4191152183,-0.2632495524
O,4.0949380972,0.4804233745,0.7765241797
O,3.92085333,0.4794580323,-1.396332459
O,-2.0916342299,-0.2376033697,0.1924497171

Cartesian Coordination of 1-3

-929.955634 hartree

C,0.0934138608,0.4927541454,-4.8550938568
C,0.3863948502,0.0104695855,-1.1782213821
C,1.7008540177,-0.0983876986,-0.7199816202
C,0.7323195645,0.8072168241,-3.6233354022
C,0.1133304169,0.0822478218,-2.6216688905
C,-0.6654038778,0.0859469516,-0.2356826993
C,-0.4376497945,0.0149487119,1.1602612169
C,0.8975938452,-0.1029164064,1.5773511499
C,-1.4981033192,0.0718148091,2.1646823452
C,-1.4132774751,-0.0392407606,3.5520038148
C,-2.718092687,0.086401502,4.0815292934
C,-3.5774467081,0.2718262446,3.0142889896
C,1.9305348238,-0.1461343822,0.6511550984
C,-0.9025337732,-0.4169304075,-4.584977547

H,-2.9996240702,0.0448356085,5.1238619016
H,-0.509564546,-0.1988934163,4.1219625106
H,-1.3765176138,-1.4250464508,-2.7864453041
H,0.3293719882,0.9020868883,-5.8269185108
H,1.5359406832,1.5137217758,-3.4711421968
H,-1.6077832006,-0.9117147976,-5.2357847448
H,1.1453614104,-0.1518091812,2.6285363764
H,-3.1753585657,0.374989792,0.9271501716
H,2.5281126405,-0.164839436,-1.4134321736
H,-4.6480612359,0.4092973341,2.9839562127
H,-1.9496859783,0.4501326748,-1.6150352789
N,3.3108689266,-0.2633808328,1.1345516129
N,-2.8351808671,0.2594223136,1.8683933687
N,-0.9155936642,-0.6408523231,-3.2250050664
O,3.492245662,-0.3292142618,2.3512594499
O,4.2116625236,-0.2884383859,0.2941685355
O,-1.9589666471,0.2360834676,-0.6676588947

Cartesian Coordination of 1^{-}-1

-929.4742291 hartree
C,1.2196670412,1.2161975043,0.0022776795
C,-0.0000064113,1.9185868016,0.0000812475
C,-1.2196764217,1.2161915411,-0.0021088068
C,-1.2569667638,-0.167653211,-0.0022024538
C,0.0000012496,-0.941783648,0.0001282054
C,1.2569646825,-0.1676472635,0.0023838534
H,2.1200936517,1.8194226482,0.0039084088
H,-2.1201073238,1.8194109313,-0.0037196868
C,2.5388790653,-0.8780733052,0.0047381216
C,2.8628749297,-2.2344391821,0.0051827123
N,3.7475102382,-0.1947565011,0.0072340461
C,4.2817520854,-2.3524559064,0.0078097847
H,2.1287026752,-3.0226849255,0.0036836187
C,4.8057628464,-1.0738009635,0.0090491796
H,3.8387615058,0.8075803962,0.0074007752
H,4.8542260091,-3.2707909974,0.008776067
C,-2.5388808266,-0.8780788054,-0.0046056137
C,-2.862882641,-2.234443267,-0.0047803445
N,-3.7475081932,-0.1947569457,-0.0074065536
C,-4.2817597217,-2.3524540832,-0.0076436837
H,-2.1287157213,-3.0226931908,-0.0029832157
H,-3.838753336,0.807580645,-0.0078575681
H,-4.8542377426,-3.2707867328,-0.0085130192
N,-0.00000929,3.3344706928,0.0000777476
O,-1.0962530535,3.9475793657,-0.001882556
O,1.0962330006,3.9475823484,0.0020363377
O,0.0000070789,-2.1952172601,0.000129529
H,5.8262285761,-0.7182186185,0.0110616044
C,-4.8057644634,-1.0737968705,-0.0092351345
H,-5.8262281955,-0.718210467,-0.011501332

Cartesian Coordination of 1^{-}-2

-929.4866029 hartree
C,-2.4600520272,-0.896742294,0.0121985384
C,4.8128710239,-1.2570349774, -0.0446914147
C,2.6117782205,-0.6822789242,-0.0218505917
C,-1.205572417,-0.1381873297,0.0043857874
C,-1.223387574,1.2488975559,-0.0206106807
C,1.2959596851,-0.0344012855,-0.0207165876
C,0.0757407691,-0.8498068691,0.0222703256
C,-0.0337200726,1.9962378959,-0.0564756266
C,-4.1529955759,-2.4239735939,0.1151507912
C,-2.7417602538,-2.2503889539,0.1900840611
C,4.0536665079,-2.418113672,0.0134372141
C,3.9089530141,-0.161379579,-0.0673514464
C,1.2129898712,1.3480671126,-0.0580197119
C,-4.7134832495,-1.1815770752,-0.1121143593
H,-4.6962995636,-3.354543349,0.2144925545
H,-3.8018006202,0.7113212487,-0.3624695108
H,2.1077236865,1.9574593865,-0.0856904541
H,-5.7409359862,-0.872549439,-0.240496692
H,1.8769022989,-2.6070374647,0.0625366012
H,5.893730514,-1.2052834659,-0.0679528884
H,4.3494891179,-3.4569229385,0.0463729273
H,-1.986957355,-3.0018142781,0.3510626305
H,-2.1487535752,1.8122274652,0.0016484714
H,4.173288042,0.8860383577,-0.1125469101
N,-3.6850008249,-0.2696425956,-0.1689030106
N,2.7359587004,-2.0521417128,0.0265284881
N,-0.0988158085,3.4179865028,-0.0849703287
O,0.9648635768,4.0762342951,-0.1088837547
O,-1.2217448532,3.976203949,-0.0874505372
O,0.1230837288,-2.117595972,0.073323115

Cartesian Coordination of 1^{-}-3

-929.498314 hartree
C,4.821159926,0.7042950899,0.0003013811
C,6.2798225074,0.6742001632,0.0010929666
C,6.9831009222,1.9524894238,0.0003991212
C,6.2639243975,3.1401062754,-0.0007259656
C,4.860968521,3.1317217276,-0.0012898581
C,4.1522282143,1.9209206706,-0.0007941977
H,6.7728630535,4.0956316089,-0.0011774054
H,3.0702506863,1.9579285195,-0.0012883222
C,4.050512694,-0.5443942796,0.0006691252
C,2.6738025821,-0.7884675375,0.0003570792
N,4.6704127903,-1.7733649744,0.0016405397
C,2.4862767976,-2.1966537917,0.0009584835
H,1.8943103804,-0.0393046773,-0.0003009359
C,3.7452669907,-2.7811224968,0.0017293781
H,5.6918606705,-1.7952985697,0.002007587
H,1.5410826736,-2.7238125953,0.0008609153
H,4.0444561042,-3.8194627385,0.0023461791
C,8.449827549,1.9955853004,0.0008751844
C,9.3495258526,3.065841653,0.0003837991
N,9.2042332316,0.8442693449,0.0019329387
C,10.6628272337,2.5241853593,0.0012589363
H,9.0904547396,4.1154779293,-0.000478045
C,10.5395363214,1.1416287427,0.0022027823
H,8.7124479472,-0.0512926789,0.0023760537
H,11.5919427177,3.0791927244,0.0011925479
H,11.2891990911,0.3633799829,0.0030362796
O,6.9231209811,-0.4400842941,0.0018807211
N,4.1454923037,4.3709624716,-0.0024262856
O,2.8963440319,4.3486971585,-0.0029466903
O,4.7893495678,5.4416233578,-0.0028777831

Cartesian Coordination of *p*-Benzoquinone

-381.4577443 hartree
C,-0.0005893709,-1.4448977708,0

C,-0.00005926,-0.6713699945,1.2693485433
C,0.0000501163,0.6713699686,1.2693486517
C,0.0001309323,1.4448977508,0
C,0.0000501163,0.6713699686,-1.2693486517
C,-0.00005926,-0.6713699945,-1.2693485433
H,0.0000539563,-1.2591982838,2.1824924503
H,0.0001874652,1.2591981855,2.1824925726
H,0.0001874652,1.2591981855,-2.1824925726
H,0.0000539563,-1.2591982838,-2.1824924503
O,0.0002764078,-2.6697915136,0
O,-0.0001275246,2.669791782,0

[S4] (Complete ref. 9)] *Gaussian 09* (Revision D.01), M. J. Frisch, G. W. Trucks, H. B. Schlegel, G. E. Scuseria, M. A. Robb, J. R. Cheeseman, G. Scalmani, V. Barone, B. Mennucci, G. A. Petersson, H. Nakatsuji, M. Caricato, X. Li, H. P. Hratchian, A. F. Izmaylov, J. Bloino, G. Zheng, J. L. Sonnenberg, M. Hada, M. Ehara, K. Toyota, R. Fukuda, J. Hasegawa, M. Ishida, T. Nakajima, Y. Honda, O. Kitao, H. Nakai, T. Vreven, J. A. Montgomery, Jr., J. E. Peralta, F. Ogliaro, M. Bearpark, J. J. Heyd, E. Brothers, K. N. Kudin, V. N. Staroverov, T. Keith, R. Kobayashi, J. Normand, K. Raghavachari, A. Rendell, J. C. Burant, S. S. Iyengar, J. Tomasi, M. Cossi, N. Rega, J. M. Millam, M. Klene, J. E. Knox, J. B. Cross, V. Bakken, C. Adamo, J. Jaramillo, R. Gomperts, R. E. Stratmann, O. Yazyev, A. J. Austin, R. Cammi, C. Pomelli, J. W. Ochterski, R. L. Martin, K. Morokuma, V. G. Zakrzewski, G. A. Voth, P. Salvador, J. J. Dannenberg, S. Dapprich, A. D. Daniels, Ö. Farkas, J. B. Foresman, J. V. Ortiz, J. Cioslowski and D. J. Fox, Gaussian, Inc., Wallingford CT, 2009.

4. Deprotonation behaviors

Spectroscopic Titrations: According to the literature procedure,[S5] the pK_a measurement (Supporting Figure 18) was conducted in a 2.5% aqueous sodium dodecyl sulfate (SDS) micellar solution of **1** with the concentration of 10^{-5} M. Nitric acid and sodium hydroxide aqueous solutions were used to adjust the pH values of the sample solutions at r.t. using a D-51 pH meter (Horiba) equipped with a 96155-10D electrode (Horiba). The ionic strength of the sample solutions was maintained at 0.2 M by adding appropriate amounts of $NaNO_3$. pK_a values of each sample were obtained from the resulting absorption plots fitted by the least-squares method.

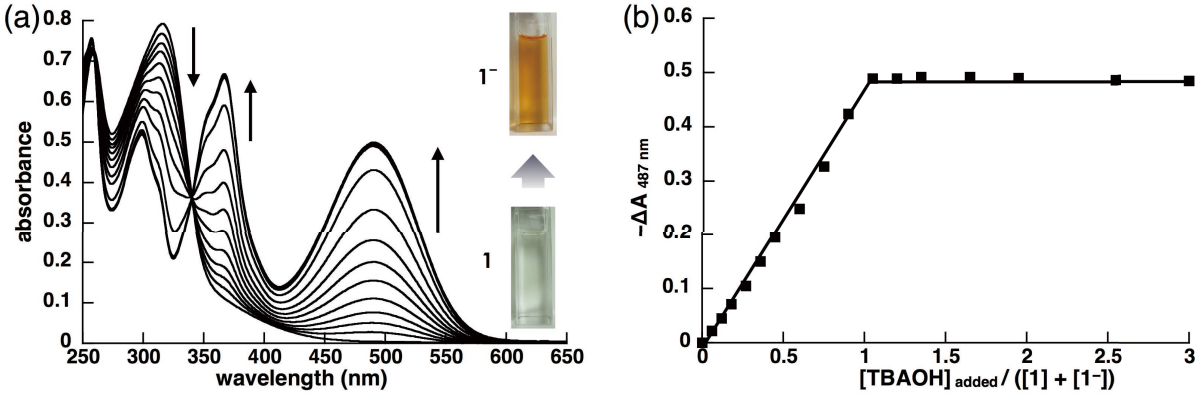

Supporting Figure 16 (a) UV/vis absorption spectral changes of **1** (6.0×10^{-5} M) upon the addition of TBAOH in CH_2Cl_2 and (b) corresponding titration plots monitored at 487 nm, suggesting that **1** can be quantitatively deprotonated to afford $\mathbf{1}^-$ by the treatment with OH^-. The titration plots monitored at 315 nm and 366 nm show the similar behaviors.

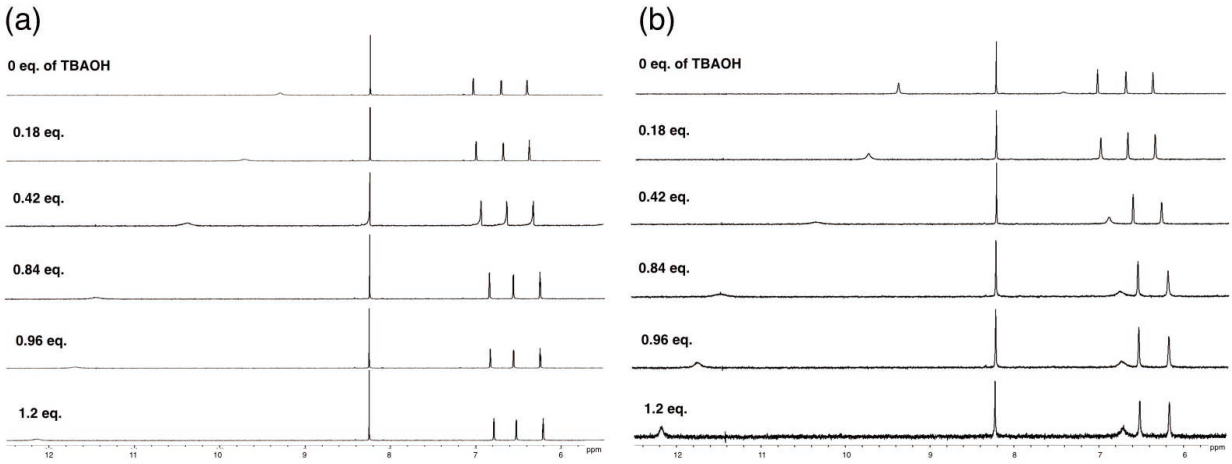

Supporting Figure 17 ^{1}H NMR spectral changes of **1** (1.1×10^{-3} M) upon the addition of TBAOH (0–1.2 equiv) in CD_2Cl_2 at (a) 20 °C and (b) –50 °C. Pyrrole NH of **1** was shifted to downfield upon the addition of 1.0 equiv of TBAOH due to the formation of hydrogen bonding with phenolate. This result suggests that the use of the bases whose pK_a values in the protonated (conjugated acid) forms are smaller than that of pyrrole NH (pK_a = 23 in DMSO) and larger than that of the hydroxy group in **1** (pK_a = 6.2, Supporting Figure 18) is important for this study. Of course, the pK_a value of the hydroxy group in **1** can be controlled by the modification of the pyrrole units. Furthermore, the pyrrole NH signal was slightly shifted to the downfield upon the addition of more than 1 equiv of TBAOH due to not only the intermolecular hydrogen bonding with the phenolate unit but also with the excess hydroxide anion. However, UV/vis absorption spectral changes (Supporting Figure 16 and 18) in dilute conditions showed only the intramolecular hydrogen bonding. In addition, the disappearance of the hydroxyl group in **1** upon the addition of a small amount of TBAOH is ascribable to the accelerated chemical exchange with the corresponding anionic form.

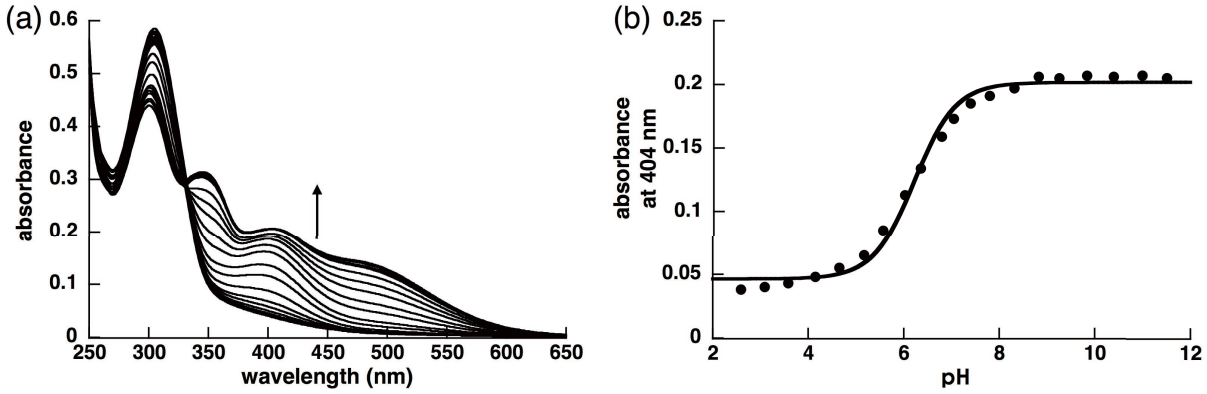

Supporting Figure 18 (a) UV/vis absorption spectral changes of **1** (10^{-5} M) in a 2.5% SDS micellar aqueous solution with 0.2 M $NaNO_3$ over the pH ranges 2.59–11.51 and (b) corresponding plots for the pH-dependent absorbance at 404 nm. The pK_a value of **1** was estimated at 6.2 ± 0.05 by the pH-dependent changes at 404 nm. Considering the estimated pK_a value of **1**, OH^- as a base is appropriate for the deprotonation because of the significantly greater pK_a value of 15.7 in their protonated form (H_2O). The absorption at 404 nm was selected for the pK_a estimation because of the large absorbance change the and also the absorption in the visible region without the significant errors derived from other factors.

[S5] R. Sakashita, M. Ishida and H. Furuta, *J. Phys. Chem. A*, 2015, **119**, 1013–1022.